Development of a highway driving events identification and classification using smartphone

Munaf Salim Najim Al-Din*

Department of Electrical and Computer Engineering,
University of Nizwa,
Nizwa, Sultanate of Oman
Email: munaf@unizwa.edu.om
*Corresponding author

Atef Saleh Al-Mashakbeh

Department of Electrical Engineering,
Tafila Technical University,
P.O. Box 179, Tafila 66110, Jordan
Email: dr.almashakbeh@gmail.com

Abstract: In recent years, the use of smartphones has grown significantly due to the increase in their computational capabilities and the integration of advanced sensor technologies. This prevalence of smartphones and advances in machine learning have greatly contributed to the field of vehicular applications in terms of accessible, available and cost. Nevertheless, the accuracy of these applications critically depends on the calibration and pre-processing techniques that is needed to mitigate these problems. This study proposes a set of simple calibration and pre-processing techniques to enhance the accuracy of a smartphone-based driving event detection and classification system. Furthermore, the paper presents a simple and effective approach for the identification and classification of driving events. The approach is based on separating the identification and the classification processes. The dynamic time warping (DTW) technique is used for the identification, while statistical and time metrics features are used for the classification. Results obtained show a high accuracy rate.

Keywords: smartphone sensors calibration; driving events detection; driving manoeuvres classification.

Reference to this paper should be made as follows: Al-Din, M.S.N. and Al-Mashakbeh, A.S. (2020) 'Development of a highway driving events identification and classification using smartphone', *Int. J. Nanoparticles*, Vol. 12, Nos. 1/2, pp.152–173.

Biographical notes: Munaf Salim Najim Al-Din is a PhD Research Scholar in the Department of Electrical and Computer Engineering at University of Nizwa, Sultanate Oman. He received his PhD in the field of Computer Aided Design Systems from the University of Technology Baghdad, Iraq, in 1997. His present work is focused on studying analysing and designing of high-efficiency vehicle driving monitoring systems. His research areas are driving behaviour analysis, robotics, machine learning and deep learning. He has more than 35 publications in various international journals and conference proceedings.

Copyright © 2020 Inderscience Enterprises Ltd.

Atef Saleh Al-Mashakbeh is an Associate Professor working at Tafila Technical University in Jordan. He obtained his PhD in Electrical Engineering from the Governmental Donesk University in Ukraine. His research interests are in the area of power quality and energy efficient systems with a focus on the smart usage of the available energy. He also worked with KADDB (King Abdullah II Design and Development Bureau - KADDB).

This paper is a revised and expanded version of a paper entitled 'Calibration and pre-processing techniques for a smartphone-based driving events identification and classification system', presented at The 2018 IEEE Electron Device Kolkata Conference (2018 IEEE EDKCON), Kolkata, India, 24–25 November 2018.

1 Introduction

The ubiquity and fast-paced development of automotive technologies and transportation systems combined with the appealing concerns in improving driving safety issues, all have urged and encouraged the study and analyses of driving behaviour. It is well known that road accidents are an everyday concern all over the world and they considered, according to the World Health Organization (2013), as the ninth cause of death in the world and they are a leading cause of fatal injuries. According to the research done in this field, it is found that drivers' errors and aggressive behaviour are the main factors that contribute to traffic accidents. On the other hand, the design and development of the new vehicular technologies such as advanced driver assistance systems, autonomous vehicles, intelligent transportation system and microscopic traffic simulation for smart cities all require an intensive knowledge and understanding of driving behaviour analysis. Therefore, several research institutes and vehicle manufacturers have initiated and invested in the development of driving behaviour monitoring and analysis systems (Wahlström et al., 2017).

In general, driving monitoring systems involve an automated collection of driving data and application of computer algorithms or models to generate a taxonomy that describes the driver behaviour and performance profile. The assessments of driving behaviours are usually performed by detecting driving events and evaluate their severity level. Such assessments require the collection of sensors data to estimate certain driving parameters, extract features and patterns for these parameters and then create a computational model to identify and classify the driving events. A wide range of sensors and algorithms have been utilised in the driving monitoring systems, ranging from the OBD data extracted from the controller area network bus, vehicle mounted cameras, customised sensors to smartphone's inertial and navigational sensors (Kaplan et al., 2015). Among this spectrum of solutions, smartphone-based vehicle driving monitoring systems are rapidly growing in number and sophistication. This shift of interest in using smartphones is contributed to the prevalence of smartphone, continuous enhancement in their computing power and integration of a variety of sensors. Furthermore, the continuous reduction of smartphones costs has encouraged the development of enormous number of applications which in turn has set a steady establishment for future mass market implementations. Nevertheless, in order to develop a reliable and accurate smartphone-based driving monitoring system, two issues need to be carefully considered, namely: the accuracy of sensors data and the validity of detection and classification algorithms (Vlahogianni and Barmpounakis, 2017).

It is best known that the core process of driving monitoring systems is the ability of estimating vehicle's dynamics by detecting, identifying and then classifying driving events accurately. Therefore, when developing a smartphone-based system a logical concern will directly rise; are smartphone's sensors able and sufficient to provide accurate estimation of vehicle's dynamics and predicts accurately driving events? As it is well known, today's smartphones are designed to contain many low-price sensors within their constrained space through the use of micro-electro-mechanical sensors (MEMS) technology. Consequently, the abundance and heterogeneity of different sensors pose several problems, for example, noise, biases, scale factors and drifts. With these impediments in the smartphone's sensors, the efficiency and the reliability in detecting and classifying driving events would greatly degrade. This fact has excited a challenging research to provide adequate remedies to these problems. These remedies in general address the calibration of sensors, noise filtering, smartphone-vehicle reorientation and accurate parameters estimations. Several methods have been introduced to tackle these problems are presented in the literature (Almazan et al., 2013; Prikhodko et al., 2018; Fida et al., 2015; Singh et al., 2017; Bruwer and Booysen, 2015), but very few have considered all of the above mentioned problems and their effects on the performance of a driving events detection and classification systems.

The second major issue in any driving behaviour monitoring and analysis system is the identification of driving actions or events and their classification. Several techniques have been suggested and used to extract features for identification and classification, for example, simple threshold discriminators (Li et al., 2017), statistical (Bejani and Ghatee, 2018), time domain analysis (Wu et al., 2016), frequency domain analysis (Lu et al., 2018), fuzzy classifiers (Aljaafreh et al., 2012, Al-Din et al., 2013) and pattern matching techniques (Al-Din, 2018). In general, the feature extraction for driving behaviour analysis can be classified as either a form of dimensionality reduction process or it is a pattern matching and recognition scheme.

This paper presents the development of a smartphone-based highway driving events identification and classification system. Two major issues are presented in this paper. The first is concerned with the calibration and pre-processing techniques that are required to enhance the quality of identification and classifications. New calibration and smoothing techniques are suggested and investigated. The calibration procedures suggested in this study includes the effects of vehicle vibration and noise. The second issue is concerned with the identification and classification processes. In this study, two features extraction schemes are used. The first is based on pattern matching scheme, while the second is used to evaluate and classify the events based on statistical and time domain metrics. This approach was found very useful since it simplifies the learning process by splitting it to identification and classification, and increases the accuracy and the reliability of the system through the segregation of the identification and classification features.

2 System architecture

The general architecture and design methodology of the proposed system is presented in Figure 1. The system consists of four main modules: raw data acquisition, pre-processing, events detection and finally events identification and classification. The function of each module is briefly described as follows:

a An Android-based smartphone is used to collect the raw data through its motion sensors namely, accelerometer, gyroscope and the magnetometer. All sensors' data are stored with a uniform sampling rate of 50 samples/second.

b The pre-processing unit is responsible of filtering collected data, sensors calibration, transformation of the real-time data to the vehicle coordinate system and finally estimates the driving parameters.

c The event detection unit, it is responsible for real-time detection and segmentation of driving events. The endpoint detection algorithm is used to identify the start and endpoints of lateral and longitudinal driving events. Short-term energy and zero-crossing rate are used as the parameters for the detector.

d The identification and classification unit is responsible for identifying the type of the event and its abnormality level. In this study, two features extraction schemes are used. The first is based on pattern matching scheme for events identification, while the second is based on statistical features and used to classify the abnormality level.

Figure 1 The proposed system architecture

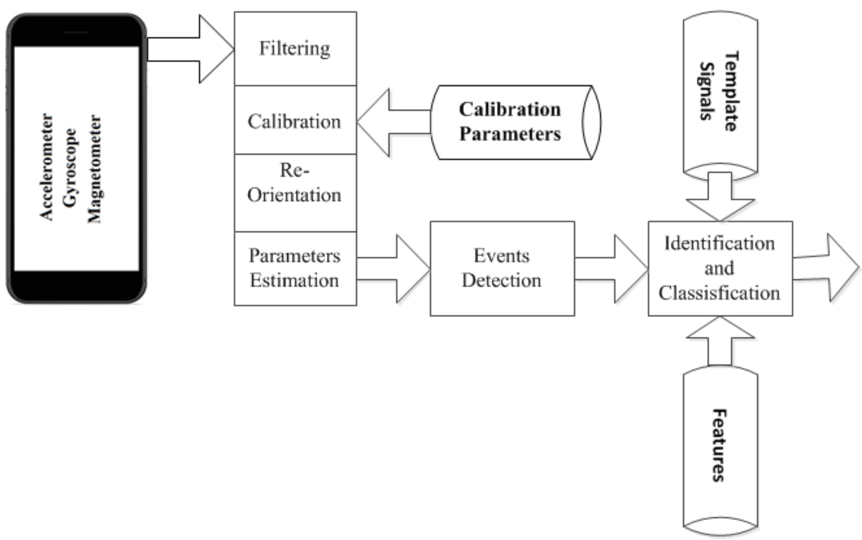

3 Sensors calibration

Sensors calibration refers to the process of correcting the deterministic errors associated with the sensors. The most common types of deterministic errors in smartphones' sensors are biases, scale factors and axes misalignment. On the other hand, sensors are also subjected to random error sources as those contributed to noise and vibration, nonlinearity due to thermal and magnetic effect and many others (Almazan et al., 2013;

Prikhodko et al., 2018). In this study, the apparently dominant errors sources, biases and scaling, will be considered in the calibration process.

3.1 Accelerometer calibration

The accelerometer usually measures the instantaneous forces acting on an object in the Cartesian coordinates. These forces are contributed to linear acceleration, gravity and noise. The general model for any accelerometer can be given by:

$$a_m(t) = S_a a_L(t) - g + b_a + n_a \tag{1}$$

Here, a_m, a_L, S_a, g, b_a and n_a represent the instantaneous measured acceleration component, the linear acceleration, scaling factor, gravitational acceleration, bias and noise, respectively.

To estimate the bias (b_a) for each of the accelerometer's components, we need first to eliminate the effects of the linear acceleration, gravity force and noise. In order to achieve this, subsequent procedure is followed in all the tests performed for estimating the biases:

a The smartphone is fixed on a flat horizontal surface so that the axis to be calibrated is in alignment with the vehicle's longitudinal direction.

b The vehicle is then driven at a constant speed over a straight road segment. Therefore, with such setup, the accelerometer can be considered in a static condition, hence it will measure the Earth's gravitational force along its vertical axis only while the other two axes would record random noise with bias.

c To eliminate the effects of the noise, a Gaussian-weighted moving average filter is used. The data obtained by the filter is then averaged to obtain an estimate for the bias for only one test.

This procedure is then repeated for the same axis but with different speeds. Figure 2 shows a sample for the measured signal along one of the smartphone's axes for a certain speed. Figure 3 shows histogram plots for the computed average for x-axis. It can be noticed from Figure 3 that the standard deviations for the measured biases are very low. Therefore, the mean value of all the averages is assumed to be the static bias for each axis.

The estimation of the accelerometer's scale factors requires slight modifications to the tests, where the speed is not constant but varies linearly. As in the estimation of the bias, the procedure is applied for each axis separately. In every test, the speed is varied from an initial value to a final value for a three second period. With this short-time, the speed can be assumed to vary linearly, and hence the acceleration will be constant. By using Newton's first law of motion, given in equation (2), the acceleration is determined. At the same time, the mean value for the measured samples is computed and used to estimate the scaling factor.

$$v_f = v_i + a_{avg} \cdot t \tag{2}$$

For the sake of simplicity, the final scale factor is computed by averaging all the estimated values. It should be noted, corrections for biases have been considered and law-pass filter is also used to smooth the measured data.

Figure 2 Unfiltered *x*-axis of accelerometer recorded data

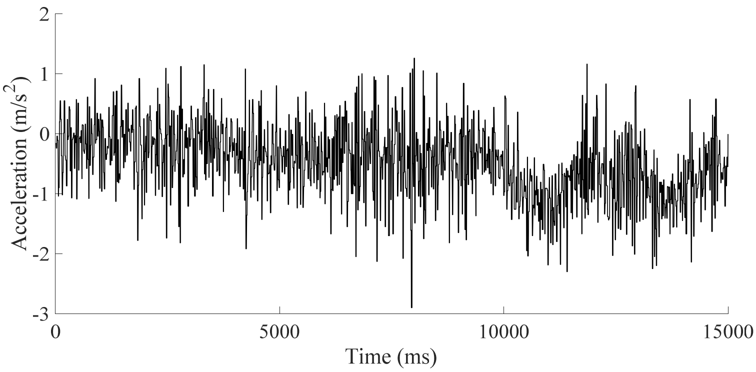

Figure 3 Accelerometer's measured biases along the *x*-axis (see online version for colours)

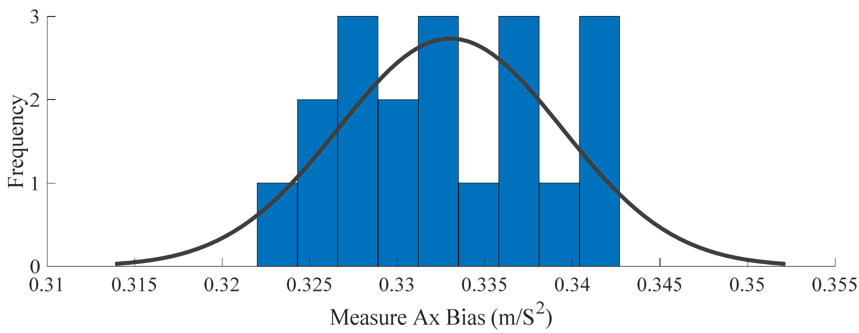

3.2 Gyroscope calibration

The gyroscope measures the rate of change of angular displacement, i.e., the angular velocity, along the smartphone's three orthogonal axes. The general model for the gyroscope is given by:

$$\omega_m(t) = S_g\omega(t) + b_g + n_g \tag{3}$$

Note that ω_m, ω, S_g, b_g and n_g represent the measured angular velocity along one of the three axes, the true angular velocity, scaling factor, bias and noise, respectively.

Starting with the estimation of the biases, the vehicle was also driven over a straight road segments with different constant speeds. In each trip, the gyroscope's axis of interest is fixed to be perpendicular to the vehicle-base surface. There are two reasons behind the adoption of such arrangement: first, the smartphone's horizontal plane is perpendicular to the gravity vector; hence the effect of gravity will be constant. Secondly, the effects of vibration, due to the vehicle and road surface, on the measurement are included. For each axis a set of measured data, about one minute each, is collected. In addition to that, the latitudes and longitudes for both the starting and ending points of the trip are also recorded. In all the considered tests the filtered accelerometers' measurements were checked to be close to zero. If any of these measurements shows more than 5% deviation from the zero value, then the test will be discarded. For each test, the mean value for the gyroscope's axial signal is calculated. Figure 4 shows the histogram plots for the measure average for the *Y*-axis. Although the variance is higher than those of the accelerometer, but still their standards of deviation are very low, hence the average of these values is considered to be the bias for that axis.

Figure 4 Gyroscope's measured biases along *y*-axis (see online version for colours)

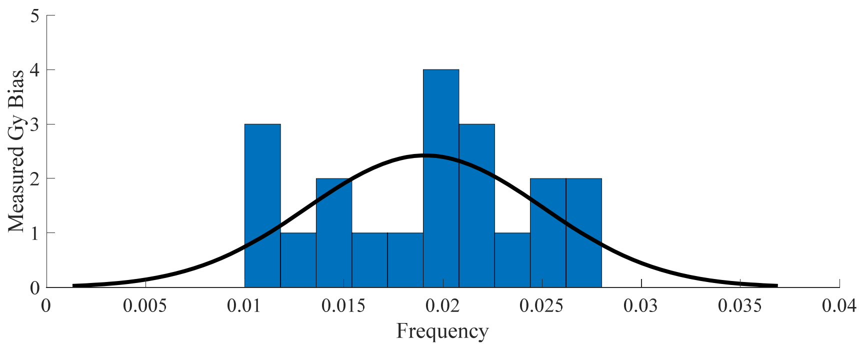

The second step in gyroscope's calibration is the determination of the scale factor. The vehicle in these tests was driven through long enough circular curved road segments. Four different road segments were chosen, each with different radius, two of them are left curved while the other two are right curved segments. As in the previous test, the latitudes and the longitudes for the starting and ending points are recorded. In each test, the speed is fixed and vehicle is driven along fixed lane. From the knowledge of the initial and final angle, the radius of the curved road then the average angular speed will be given by:

$$\omega_{avg} = \frac{\Delta\theta}{\Delta t} \tag{4}$$

Each test, fixed speed on the same segment, is repeated several times. Note that correction of the bias is taken into consideration. As in the case of the accelerometer, the average value for the measured angular velocity is first computed and then compare to that obtained from equation (4). From these two values, an estimate for the scale factor is found. The test is repeated for each road segment with different speed and the computed scale factors are then used to determine the final scale factor.

3.3 Magnetometer calibration

Magnetometers measure the surrounding magnetic field, i.e., the external and Earth's magnetic fields. Therefore, when there is no magnetic disturbance present, the magnetometer measures only the Earth's magnetic field, which points to the North Pole, hence it can be used for heading estimation. In addition to the biasing problem, other disturbances such as soft and hard iron losses and the surrounding fields, add to the noise component in the general model of the magnetometer axial signal model. Only the effect of the bias is considered in this study. The vehicle in these tests was driven at constant speed along the four circular curved road segments as those of the gyroscope's tests.

Similarly, the smartphone is fixed on a flat horizontal surface so that the axis of interest is in alignment with the vehicle's vertical direction, and the latitude and longitude of the starting and ending points are recorded. There is no need to rotate the smartphone in these tests, since the vehicle is changing its direction continuously. For each test, the least-squares ellipsoid fitting is used to extract the vector of the local Earth's magnetic field (Kok and Schon, 2016). The final local Earth's magnetic field used in the calibration is obtained by average all the direction vectors obtained from this set of tests.

4 Pre-processing

The pre-processing unit is a collection of modules that aim to overcome in real-time four major problems: filtering the raw sensors data, calibrating measured raw data, the reorientation of smartphone with respect to the vehicle reference frame and finally estimating the real-time driving parameters.

4.1 Filtering

In addition to the deterministic errors, smartphone's sensors' models contain an additive noise term. Usually induced noise signals fluctuate very rapidly and mostly have zero mean value. Therefore, data collected from the sensors are distorted with white noise, which is simply a sequence of zero mean uncorrelated random samples. Figure 2 shows a sample for the measured accelerometer's *X*-axis signal. To prevent the noise from having an apparent influence on the parameters estimation, an effective filtering is required. There are different methods to smooth or filter noisy signals, for example, statistical filters (Pan et al., 2016), digital filters (Singh et al., 2017), Kalman filter (Wu et al., 2016) and many others. Two types of filters have been investigated and used in this study, Kalman and statistical filters.

Kalman filter is an algorithm that recursively minimises the mean square error to calculate the best estimate of a signal when embedded with noise. It processes samples as they arrive and computes a new state in each cycle depending only on previous state estimate and the new input data. Although that Kalamn filter proved to be very accurate and reliable technique, but its main drawback is complexity of its implementation. Statistical filters like moving average, exponential, Savitzky-Golay, and many other specialised smoothing techniques, are found to be simpler in implementation and execute faster. Several statistical smoothing techniques were tested and it is found that the locally weighted smoothing technique (LOESS). The LOESS technique is usually used in regression analysis in which it creates a smooth line between the dependent and independent variable. The detailed theory and implementation of this technique can be found in Martinez and Martinez (2005). Since the measurement of the real signals and the separation of noise are not possible because of randomness of the road and vehicle conditions, a sinusoidal signal with additive noise is used to evaluate the performance of the three filtering methods. Figure 5 shows the results obtained for the three techniques; note that the noise signal is represented by dots and the filtered signal by solid line. It is clear that the LOESS technique can achieve very close results to Kalman filter. Figure 6 shows the filtered signal for an actual accelerometer sensor raw data.

Figure 5 Filtering results for test signal, (a) original signal (b) moving average (c) LOESS (d) Kalman filter (see online version for colours)

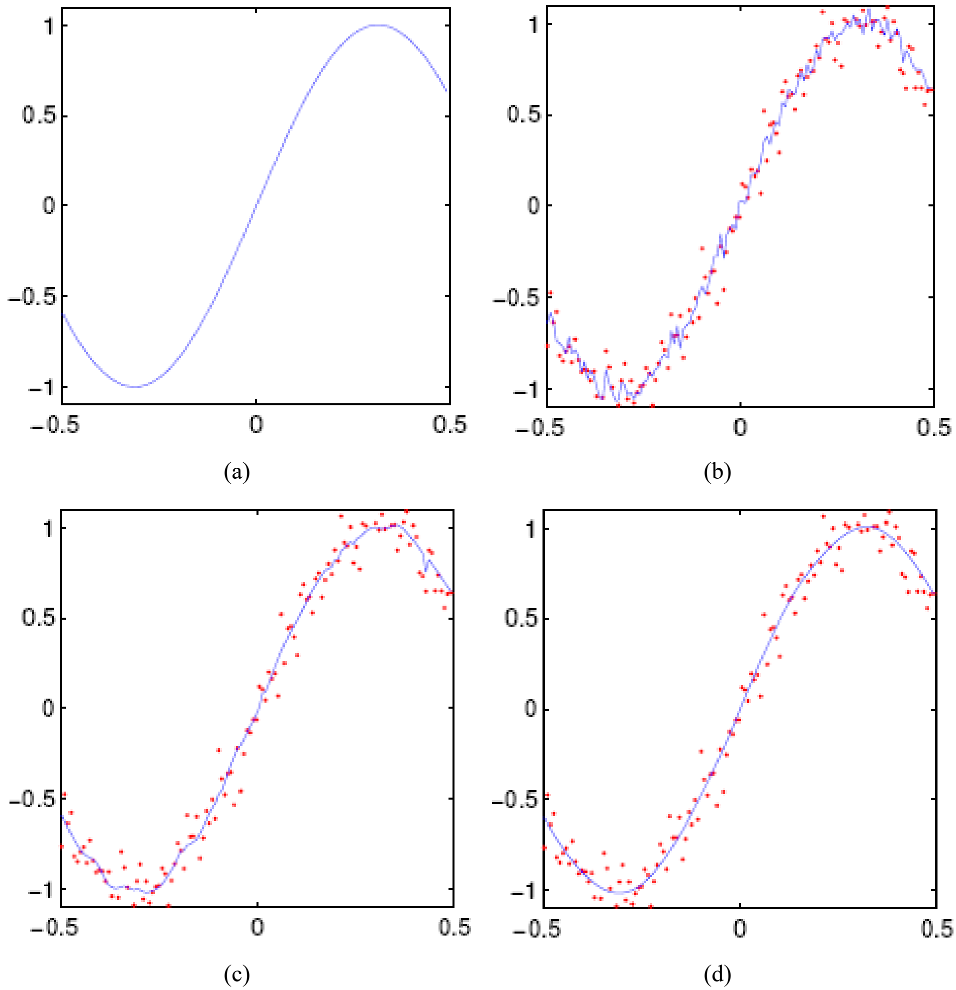

4.2 Smartphone reorientation

When smartphones are used to detect vehicle's dynamics, they could be placed within the vehicle in any orientation. In this study, the smartphone is affixed to the windshield by a holder. As a consequence of this placement arrangement, the coordinate systems of both the phone and the vehicle are not aligned. Therefore, a reorientation process for the smartphone's coordinate systems is required to transform the measured sensors data to the vehicle coordinate system. This process can be performed through a sequence of basic geometrical rotations using Euler angles as shown in Figure 7.

Figure 6 Raw and filtered accelerometer data (see online version for colours)

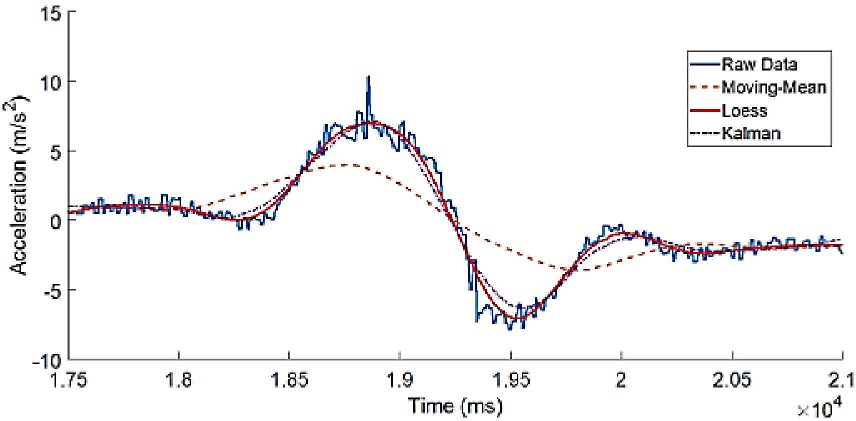

Figure 7 Smartphone and vehicle coordinate systems (see online version for colours)

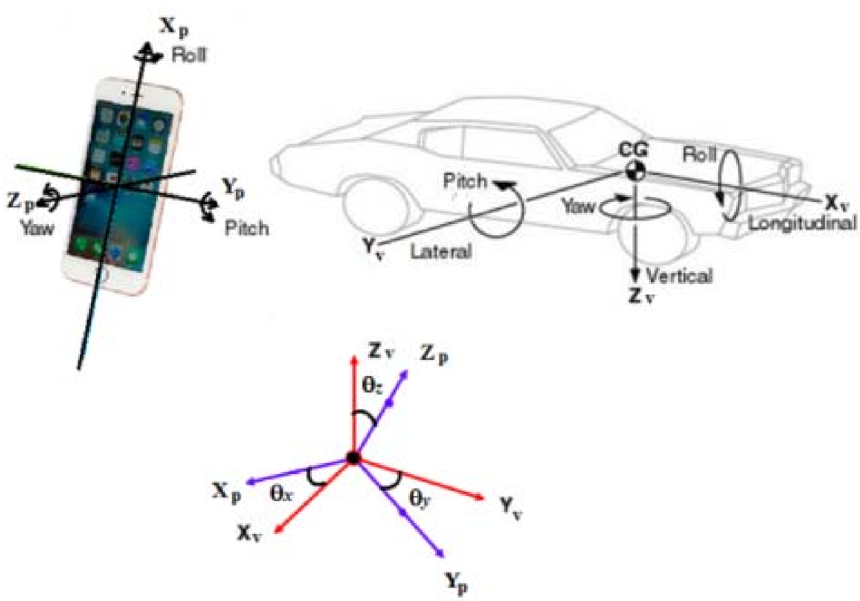

The procedure used to determine these angles is adopted from Bruwer and Booysen (2015). Once these rotational angles are obtained, the phone referenced coordinate system can be transformed into the vehicle-referenced coordinate system by multiplying with the reorientation matrices as follows:

$$\begin{bmatrix} f_{xv} \\ f_{yv} \\ f_{zv} \end{bmatrix} = \mathbb{R} * \begin{bmatrix} f_{xp} \\ f_{yp} \\ f_{zp} \end{bmatrix} \tag{5}$$

where f_{iv} is the transformed measured signal to the vehicle reference, f_{ip} the measure signal in the phone reference and R is rotation matrix defined by:

$$\begin{aligned}\mathbb{R} &= R(\theta_x) * R(\theta_y) * R(\theta_z) \\ &= \begin{pmatrix} 1 & 0 & 0 \\ 0 & \cos\theta_x & \sin\theta_x \\ 0 & -\sin\theta_x & \cos\theta_x \end{pmatrix} * \begin{pmatrix} \cos\theta_y & 0 & -\sin\theta_y \\ 0 & 1 & 0 \\ \sin\theta_y & 0 & \cos\theta_y \end{pmatrix} * \begin{pmatrix} \cos\theta_z & \sin\theta_z & 0 \\ -\sin\theta_z & \cos\theta_z & 0 \\ 0 & 0 & 1 \end{pmatrix}.\end{aligned} \tag{6}$$

4.3 Driving parameter

In this study, the driving parameters used to estimate vehicle's dynamics and driving events are: speed, longitudinal and lateral accelerations and yaw for orientation. It is believed that the selection of these parameters and not the sensors data would be more informative and useful in the analysis.

The first parameter estimated is the vehicle's heading. Euler angles namely: yaw, pitch and roll, are usually used to describe the vehicle's orientation. The three angles can be estimated directly by integrating the gyroscope's measured signals (Huang et al., 2015). Also, they can be obtained by using both the accelerometer and the magnetometer, in which the accelerometer can be used to estimate the roll and the pitch and the magnetometer can be used to estimate yaw by using simple trigonometric projections. Nevertheless, both approaches suffer from certain limitations that affect the accuracy of the estimation. For example, gyroscope suffers from stochastic bias variation which causes an accumulated drift error (Huang et al., 2015). On the other hand, both accelerometers and magnetometers are very sensitive and their signals are very noisy.

To address these limitations in both approaches, sensor fusion approaches are developed and widely adopted by many researchers. The objective of sensor fusion is to combine the data from all the sensors and then compensate the weakness of one sensor with the strength of the others. Kalman and complementary filters are two widely used sensor fusion techniques used to determine the vehicle orientation. In this study, the complementary filter is used for the determination of the orientation because of it is simplicity and reliability. Figure 8 shows the general structure of a complimentary filter. The filter combines the accelerometer and magnetometer estimation with the gyroscope estimation.

The complementary filter applies low-pass filters on both the accelerometer and the magnetometer singles to eliminate the effects of noise and dynamic bias, while employ a high-pass filter on the gyroscope's signals to suppress the drift. The filter is then estimates the angles by using the following equation:

$$\theta_i = \alpha\left(\theta_{i-1} + \Delta\theta_{gi}\right) + (1-\alpha)\theta_{a,mi} \tag{7}$$

Here, θ_i is the estimated angle, roll, pitch or yaw, θ_{i-1} previously estimated angle, the subscripts g, a and m indicates the used sensor, finally, α is an empirical factor that sets the time constant at which the error-signal calculations stabilise the rate-sensor angle calculation. It should be noted that the time constant for the two filters is set to be longer than the expected manoeuvres in testing.

Longitudinal and lateral accelerations can be estimated directly from the accelerometer's Cartesian components, a_{vx}, a_{vy} and a_{vz}. Once these measured components are transformed from the smartphone's to the vehicle's coordinate system, the planer components are then used to compute the lateral and longitudinal acceleration components as follows:

$$a_{lat} = a_{vx} \sin\gamma + a_{vy} \sin\rho \tag{8a}$$

$$a_{lon} = a_{vx} \cos\gamma + a_{vy} \cos\rho \tag{8b}$$

where a_{lat} and a_{lon} are the lateral and longitudinal components and ψ and ρ are defined by:

$$\gamma = \cos^{-1}\frac{a_{vx}}{\sqrt{a_{vx}^2 + a_{vy}^2}} \text{ and } \rho = \cos^{-1}\frac{a_{vy}}{\sqrt{a_{vx}^2 + a_{vy}^2}} \tag{9}$$

The last parameter used in this study is the speed. Trapezoid rule is used to integrate the estimated longitudinal acceleration to obtain speed as given in equation (10):

$$v_i = v_{i-1} + \frac{1}{2}(a_{i-1} + a_i) \tag{10}$$

where v_i is the current estimated speed and v_{i-1} is the previously estimated value.

Figure 8 Block diagram of digital complementary filter (see online version for colours)

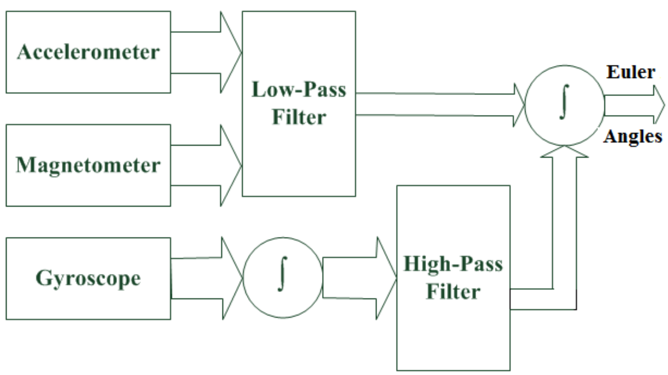

5 Feature extraction and classification

In order to develop a reliable and accurate identification and classification model, an adequate dataset for various driving events need to be generated. In this study, ten drivers with different vehicles volunteered to drive through a highway road section of 15 km long shown in Figure 9. In order to have sufficient data for training and testing, each driver is asked to repeat five times each of the basic divining events: acceleration, braking, left lane change, right lane change, merging and exiting the highway. The first four events were performed on both straight and curved road segments. Data collected from these tests are first pre-processed and then segmented to extract label the events. Two cars digital video recording cameras were installed to record the state of the vehicle and the driver. The extracted driving events combined with video recording were combined and presented for inspection and evaluation by three experts, to classify the abnormality level of the events.

Figure 9 The route used to collected training data (see online version for colours)

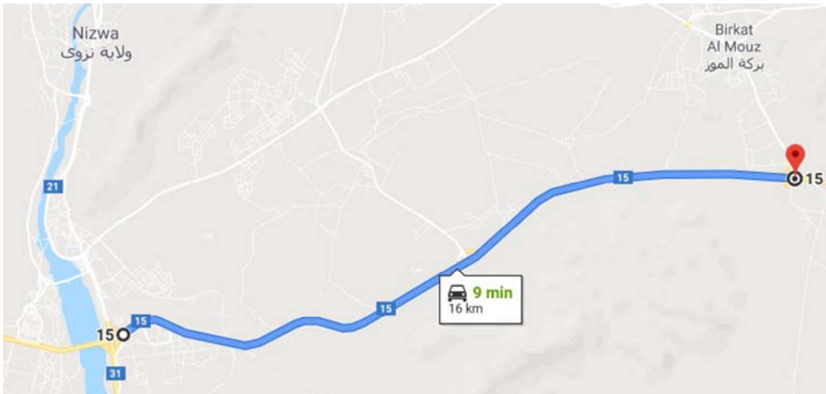

In this study, two features extraction schemes are used. The first is based on pattern matching scheme to identify the type of the event, while the second is based on dimensionality reduction and used to evaluate and classify the event abnormality level. This approach is found to be very useful since it simplifies the learning process and increases the accuracy and the reliability of the system through the segregation of the identification and classification features.

5.1 Driving events identification

Driving events identification is concerned with the recognition of the event's type. By conducting intensive observations on the driving parameters' time variations, it was noticed that the signals share common patterns or signatures. Therefore, this feature is used to distinguish between the events. Figure 10 shows these common patterns for all the investigated events. Based on this finding the pattern matching classification scheme dynamic time warping (DTW) is used for events identification.

The DTW is a mathematical pattern matching technique which allows the comparison of two signals that may endure different duration by measuring the similarity between them. The technique has earned its reputation by being an efficient similarity measure scheme for signals that reduces the effects of shifting and distortion in time by allowing flexible transformation to detect similar shapes with different phases. The similarity measure is usually expressed in terms of distance function like the Euclidean distance between the two signals. The two signals that are usually used in a DTW implementation are the reference signal $R = \{r_1, r_2, \ldots, r_m\}$ and an unknown signal $S = \{s_1, s_2, \ldots, s_n\}$ that need to identified through its pattern shape. The DTW technique utilises dynamic programming approach to build an adjacency matrix $D(m \times n)$, as shown in Figure 11, to find the shortest warping path $P = \{p_1, p_2, \ldots, p_k\}$.

Each element $D(i, j)$ of this matrix is linked with the squared Euclidean distance defined by:

$$d(r_i, s_j) = (r_i - s_j)^2 \tag{11}$$

While the length of the warping path k is given by:

$$\max(m, n) \leq k < m + n \tag{12}$$

Figure 10 Common driving parameters' patterns (see online version for colours)

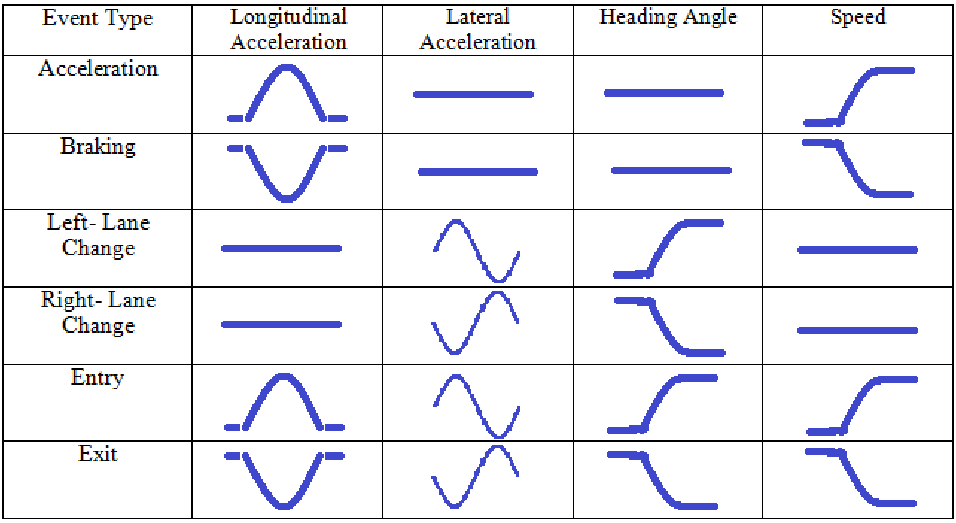

Figure 11 A DWT matrix with a warp path (see online version for colours)

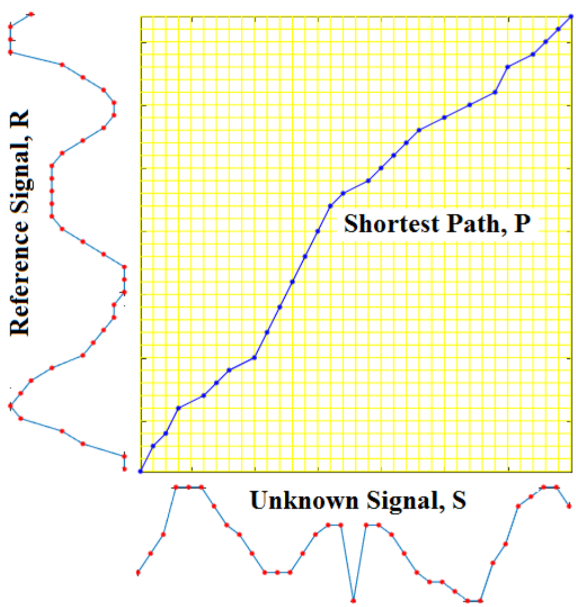

It should be noted that the warp path must start at the beginning, for each signal, at $p_1 = (1, 1)$ and finishes at $p_k = (m, n)$. The minimum distance between the two signals can be found by searching for a path in the matrix that minimise the sum of local distances encountered from the start point $p_1 = (1, 1)$ to the endpoint $p_k = (m, n)$. The optimum can be obtained by calculating the accumulated distance $D(i, j)$ for each entry (i, j) as:

$$D(i, j) = \begin{cases} d(1, 1), & \text{if } i = j = 1 \\ d(i, j) + \min\{D(i-1, j), D(i, j-1), D(i-1, j-1)\}, & \text{otherwise} \end{cases} \tag{13}$$

Once the accumulated cost matrix is obtained, the warping path could be found by the simple backtracking from the point $p_k = (m, n)$ to the $p_1 = (1, 1)$. The linear memory parallelisation schemes based on the CUDA-enabled accelerators is used to find the shortest warp path as shown in Figure 12 (Martinez and Martinez, 2005).

Figure 12 Parallelisation scheme of constrained DTW (see online version for colours)

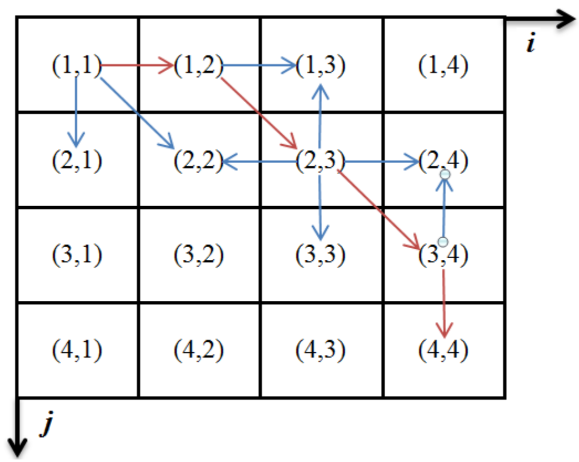

In order to identify the events by the DWT technique, a set of pre-recorded reference signals for each event are required as reference signals or so called templates. Usually, these reference templates are selected from the collected training signals based on experience or by averaging similar signals. The later approach is adopted in this study to extract the template signal for each event class. The main problem in using the averaging approach is that it is not possible to compare and merge the signals by simple averaging techniques because they have different durations and amplitudes. Therefore, they have to be nonlinearly compared in time. In this study, each signal, for specific event class, is first assumed to be the reference signal for a DTW module. The similarity measures between the pivot signal and the others are then computed. This process is then repeated for all the available signals of the event's class. The signal that will have the minimum value of the average of the similarity measures is then selected as a reference template for future classification.

5.2 Driving events classification

The classification of driving events is the process that evaluates the event's anomaly level. Statistical and time metrics have been used for evaluating event's anomaly level. Each event is classified into one of three classes namely: hard, normal and light. By reconsidering Figure 10, it can be noticed that all the signals can be classified into one of seven distinguishable patterns. Based on this fact, the time metrics for each pattern were defined as shown in Figure 13. Note that the seventh pattern is omitted since it has no significance because it is just constant value. On the other hand, basic statistical features namely: max., min., mean, standard of deviation and the variance are used. For every driving event sample, the statistical and the time metrics for each driving parameter are extracted and stored as a vector. The labelling of the event, as it has been mentioned previously, is based on the judgment made by three experts. Each expert was given an evaluation form to scale the abnormality level of driving event sample. If all the evaluation of the event came in a close agreement, then this event is taken as a training sample for the classifiers, otherwise if the there is a significant disagreement between experts' evaluations, then the sample is discarded from the training sets. It is should be noted that the percentage of the rejected samples was less than 10%.

Figure 13 Time metrics for the common signals (see online version for colours)

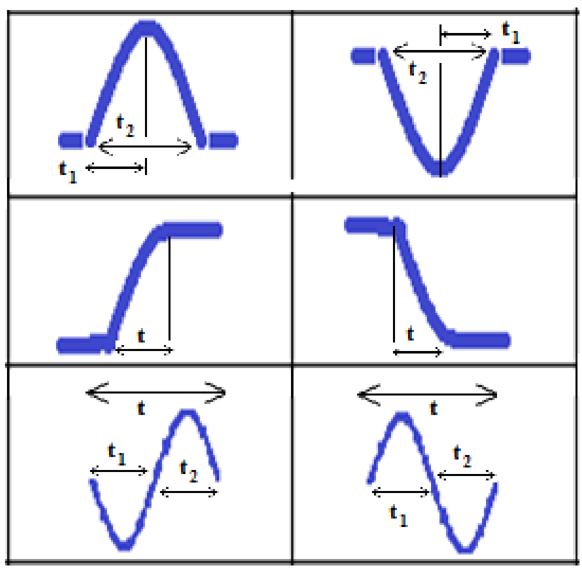

5.3 Classification model

Classification is a supervised machine learning approach used to train a model by using a number of samples belonging to a certain class. The resulted model is then used to predict new unseen samples. As been stated previously in this steady the event identification is separated from the event's evaluation. Therefore, a two stages classifier is used for the identification and evaluation. In the first stage, all the similarity distances computed by the four DTW modules are used to train a feed-forward neural network (FFNN) classifier. The main tasks of this FFNN classifier, during real-time operation, is to identify the type of the event and to trigger one of the ten FFNNs used for the evaluation of the event, note that all possible events types are summarised in Table 1. The evaluation stage is made from ten simple FFNNs, each one is used to evaluate the abnormality level for a specific event class. The statistical and time metrics for each event class are used to train one of these ten FFNNs. From these input vectors, the networks classify the respective event into three classes, hard, normal and light.

Table 1 Basic event classes

1	Acceleration straight road segment	2	Acceleration curved road segment
3	Braking straight road segment	4	Braking curved road segment
5	Left lane change straight road segment	6	Left lane change curved road segment
7	Right lane change straight road segment	8	Right lane change curved road segment
9	Merging into highway	10	Exit from highway

6 Driving event detection

Generally, one of the major problems that affect the efficiency of any driving monitoring system is the detection of a driving event. In this paper, the real-time captured data are first pre-processed and then segmented to non-event and event segments by an event detection module. The endpoint detection algorithm is used for event detection. In order to detect the endpoints of those events, short-term energy is used to distinguish an event from a non-event segment. It is noteworthy to mention here that only the longitudinal and lateral acceleration signals are used for the detection of all the events.

Basically, the module is divided into three major stages. In the first stage, the signal is segmented into non-overlapping windows of a 100 ms width. For each window, the short-time energy is first computed for the discrete data contained within the window. The value is then compared to a threshold, if energy is less than a defined threshold, then this frame is discarded and assumed to be a non-event segment. Otherwise, if the energy exceeds a lower threshold T_l then the execution of the second stage will be triggered. It should be noted that the value of the threshold depends on the type of the detected event.

Upon the triggering of the second stage, the event's start time is recorded and the short-time energy is computed over a sliding rectangular window function. The short-time energy of a discrete signal is then given by:

$$E_w = \sum_{m=n-N+1}^{n} \left[f(m) W(n-m) \right]^2 \tag{14}$$

Here, $W(n - m)$ represents a rectangular window function, N is the window's length, and the value ranges of n are 0, L, …, kL, in which L is the sliding part length. Note that the rectangular window function is defined as:

$$W = f(m) = \begin{cases} 1, & 0 \le n < N-1 \\ 0, & \text{otherwise} \end{cases} \tag{15}$$

The outcome of this stage could lead to one of the following possibilities:

- If the short-term energy is kept less than the upper threshold T_u for more than two seconds or the energy dropped back to a level lower than T_l, then this segment is considered as a non-event segment. The execution will start again from Stage 1.
- For the second possibility, if the energy will go higher than an upper threshold T_u for at least one second, then this segment will be considered as an even segment. The

system then will continue compute and compare the energy until it fall back to be lower than T_l again. Nevertheless, if the energy is dropped below T_u before the elapsing of the first second and last for half second, then this segment will be considered as a non-event segment, and the execution will start again from Stage 1. Figure 14 shows the variation of the longitudinal acceleration signal and illustrates the detection process.

Figure 14 Event detection of driving events (see online version for colours)

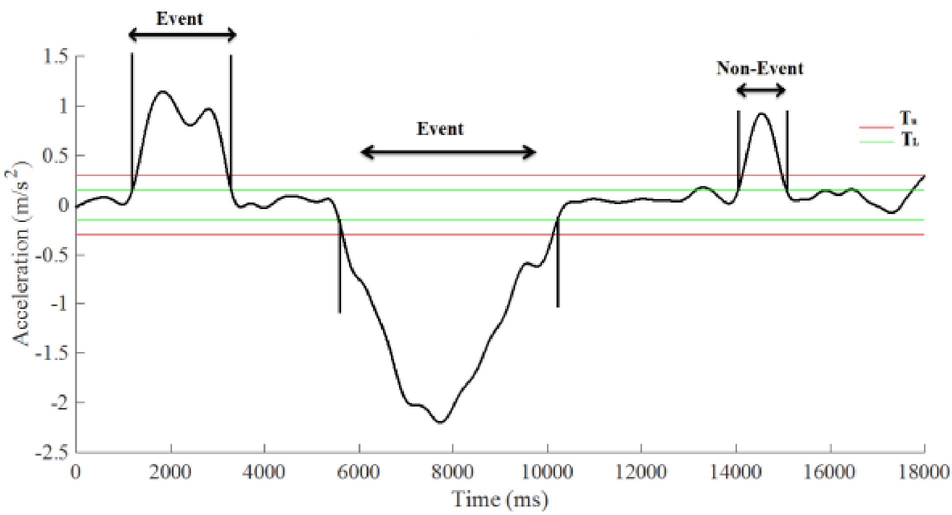

7 System validation

For testing the validity of the system, three different testing levels are performed. The first is to check the validity and accuracy of the estimated driving parameters. The second test used to check events identification and classification rate. Finally, real-time tests conducted and used to check the overall performance of the system.

To validate the accuracy of the proposed calibration and pre-processing techniques, the estimated speed is compared with the velocity measured directly through the CAN-BUS by using a Bluetooth enabled OBD-II interface. Figure 15 shows a comparison between the measure and estimated speed.

The initial training of the neural networks was done using the machine learning software WEKA. Only 60% of the examined samples were used to extract the feature vectors that used to train the neural networks. The other 40% were used to validate the accuracy of the system. Figure 16 shows results obtained when the 40% testing samples fed to the identification module. It can be seen clearly that the identification rate is close to 100%, and this is obvious since the identification process combines all the similarities for the four parameters. Figure 17 shows the rate of correct and false classification for the 40% testing samples. Again, it can be noticed that the classification rate is very high approaching 96% for some cases. This high identification and classification rates are expected since the two processes have been separated.

Figure 15 Measured and estimated speed (see online version for colours)

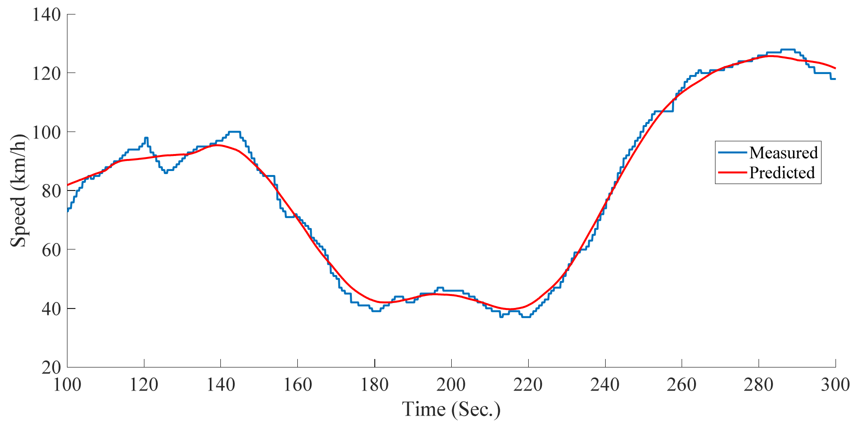

Figure 16 Events identification rate for the 40% testing samples (see online version for colours)

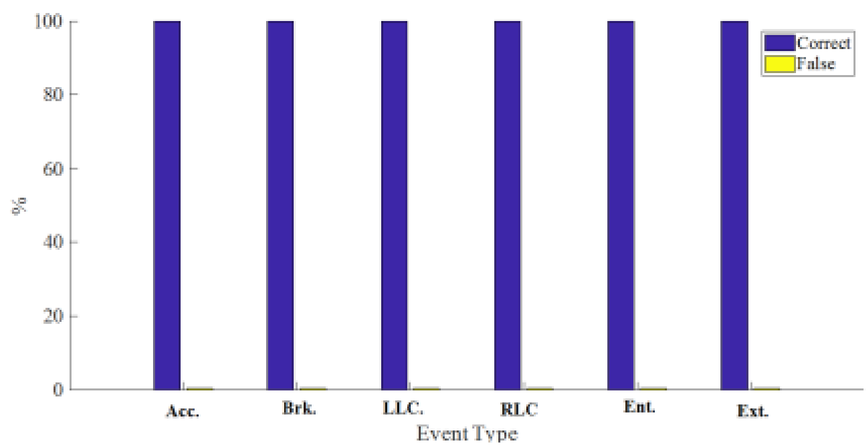

The final real-time version of the system is installed on a Samsung Galaxy S5 smartphone and used to record and analyse the trips conducted by the ten volunteered drivers. The trips were conducted with different vehicles and through different highway road sections. In addition to the system's automatic identification and classification events, manual recording of these events were also stored for the future evaluation. Figure 18 shows a comparison between the correct and false classification rate for each the driving events recorded in all the practical tests.

Results obtained in this investigation show an identification rate approaching 100%, while the classification rate is as close as to 95%. Such high identification and classification rate is considered very promising when compared to results obtained by different researchers, for example, Al-Din et al. (2013) achieved an accuracy of 84% when using a decomposed fuzzy logic system, while Pholprasit et al. (2015) an accuracy of 75% is achieved when using the DTW technique for the accelerometer with magnetic produces, finally Ming et al. (2017) achieved an accuracy of 79.4 when the authors used use both the OBD-II and mobile phone sensor data.

Figure 17 Events classification rate for the 40% testing samples (see online version for colours)

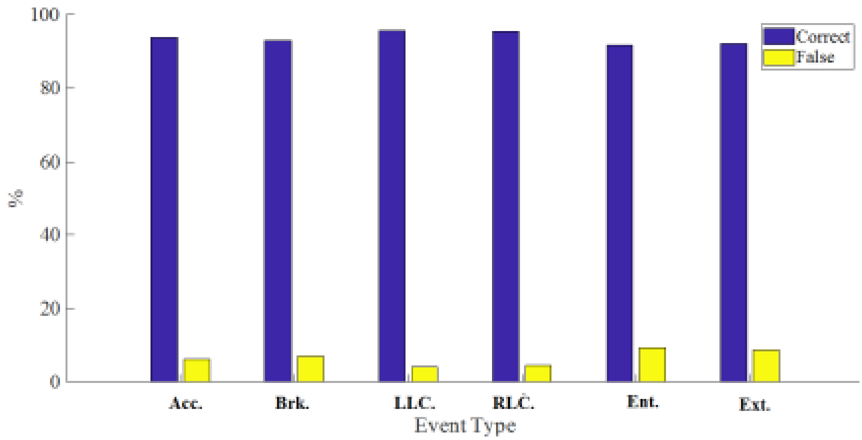

Figure 18 Events classification rate for the real-time trips (see online version for colours)

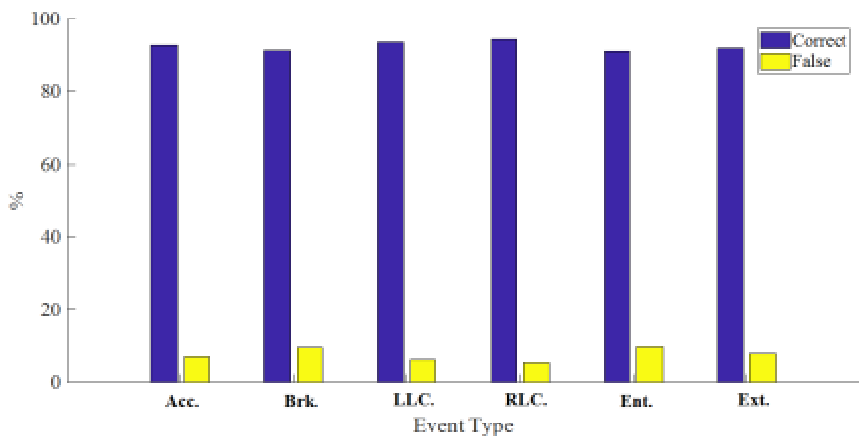

8 Conclusions

This paper proposed a smartphone-based highway driving events identification and classification system. The development of the system is totally based on the smartphone's sensors. Usually, these sensors suffer from many problems such as noise, biases, scale factors and drifts. Furthermore, the measurement process is subjected to a high degree of uncertainty. Therefore, these sensors would not be reliable to predict accurately driving events unless an effective calibration and filtering procedures are employed. A novel calibration procedure have been suggested and used in this study. Tests required for the smartphone's sensors calibration were conducted in real-time driving trips to include the vibration due vehicle and road roughness. The statistical LOESS filtering technique is used to filter sensors' high-frequency noise. Filter's performance is very close to Kalman filter performance, but it is simple to implement and faster in execution. The proposed calibration and filtering procedures were found to greatly enhance the identification and classification of the driving events.

The second part of paper proposed a novel driving events identification and classification system. The classification process for driving events in this study has been separated into identification and classification processes. This approach is found to be very useful since it simplifies the learning process and increases the accuracy and the reliability of the system through this separation of the two processes. It was noted that driving parameters for each event class have common patterns, thus the DTW technique is used for the identification. The linear memory parallelisation schemes based on the CUDA-enabled accelerators is used to find the shortest warp path. A single FFNN is trained to take the similarities for the four driving parameters to identify the type of the event and to trigger the required classification module. Statistical and time metrics features were used for evaluating event's abnormality level. The labelling of the training samples is based on the full agreement of three experts' evaluation. In the classification process ten FFNNs were employed, each one is trained for specific event class. Both offline and real-time results proved the effectiveness of this technique.

Results obtained in this investigation show an identification rate approaching 100%, while the classification rate is as close as to 95%. The classification process for driving events in this study has been separated into identification and classification processes. The DTW technique is used for the identification, while statistical and time metrics features used for evaluating event's abnormality level. Results obtained shows excellent identification and evaluation rate.

References

Al-Din, M.N., Aljaafreh, A., Albdour, N. and Saleh, M. (2013) 'Driving styles recognition using decomposed fuzzy logic system', *International Journal of Electrical, Electronics and Computer Systems (IJEECS)*, Vol. 16, No. 1, pp.820–824.

Al-Din, M.S.N. (2018) 'Calibration and pre-processing techniques for a smartphone-based driving events identification and classification system', *The 2018 IEEE Electron Device Kolkata Conference*.

Aljaafreh, A., Alshabatat, N. and Al-Din, M.S.N. (2012) 'Driving style recognition using fuzzy logic', *2012 IEEE International Conference on Vehicular Electronics and Safety*, Istanbul, Turkey, pp.460–463.

Almazan, J., Bergasa, L.M., Yebes, J.J., Barea, R. and Arroyo, R. (2013) 'Full auto-calibration of a smartphone on board a vehicle using IMU and GPS embedded sensors', *2013 IEEE Intelligent Vehicles Symposium (IV)*, Gold Coast, Australia, pp.1374–1380.

Bejani, M.M. and Ghatee, M. (2018) 'A context aware system for driving style evaluation by an ensemble learning on smartphone sensors data', *Transportation Research Part C*, April, Vol. 89, pp.303–320.

Bruwer, F. and Booysen, M. (2015) 'Vehicle acceleration estimation using smartphone-based sensors', *34th Annual Southern African Transport Conference (SATC 2015)*, Pretoria, South Africa, pp.118–129.

Fida, B., Bernabucci, I., Bibbo, D., Conforto, S. and Schmid, M. (2015) 'Pre-processing effect on the accuracy of event-based activity segmentation and classification through inertial sensors', *Sensors*, Vol. 15, No. 9, pp.23095–23109.

Huang, Y-H., Rizal, Y. and Ho, M-T. (2015) 'Development of attitude and heading reference systems', *Proceedings of 2015 International Automatic Control Conference (CACS)*, Yilan, Taiwan, pp.13–18.

Kaplan, S., Guvensan, M.A., Yavuz, A.G. and Karalurt, Y. (2015) 'Driver behavior analysis for safe driving: a survey', *IEEE Transactions on Intelligent Transportation Systems*, Vol. 16, No. 6, pp.3017–3032.

Kok, M. and Schon, T.B. (2016) 'Magnetometer calibration using inertial sensors', *IEEE Sensors Journal*, Vol. 16, No. 14, pp.5679–5689.

Li, Y., Xue, F., Feng, L. and Qu, Z. (2017) 'A driving behavior detection system based on a smartphone's built-in sensor', *International Journal of Communication Systems*, Vol. 30, No. 8, pp.1–13.

Lu, D-N., Nguyen, D-N., Nguyen, T-H. and Nguyen, H-N. (2018) 'Vehicle mode and driving activity detection based on analyzing sensor data of smartphones', *Sensors*, Vol. 18, No. 4, pp.1036–1061.

Martinez, W.L. and Martinez, A.R. (2005) *Exploratory Data Analysis with MATLAB*, Chapman & Hall/CRC Press, Florida, USA.

Ming, L.J., Tan, I.K.T. and Hoong, P.K. (2017) 'Classifying drivers using electronic logging devices', *2017 Fifth International Conference on Information and Communication Technology (ICoICT)*, Malacca City, Malaysia, pp.1–5.

Pan, T-Y., Kuo, C-H. and Hu, M-C. (2016) 'A noise reduction method for IMU and its application on handwriting trajectory reconstruction', *2016 IEEE International Conference on Multimedia & Expo Workshops (ICMEW)*, Seattle, WA, USA, pp.1–6.

Pholprasit, T., Choochaiwattana, W. and Pundit, D. (2015) 'A comparison of driving behaviour prediction algorithm using multi-sensory data on a smartphone', *2015 IEEE/ACIS 16th International Conference on Software Engineering, Artificial Intelligence, Networking and Parallel/Distributed Computing (SNPD)*, Takamatsu, Japan, pp.2267–2270.

Prikhodko, I.P., Bearss, B., Merritt, C., Bergeron, J. and Blackmer, C. (2018) 'Towards self-navigating cars using MEMS IMU: challenges and opportunities', *2018 IEEE International Symposium on Inertial Sensors and Systems (INERTIAL)*.

Singh, G., Bansal, D. and Sofat, S. (2017) 'A smartphone based technique to monitor driving behavior using DTW and crowdsensing', *Pervasive and Mobile Computing*, Vol. 40, No. C, pp.56–70.

Vlahogianni, E.I. and Barmpounakis, E.N. (2017) 'Driving analytics using smartphones: algorithms, comparisons and challenges', *Transportation Research Part C*, June, Vol. 79, pp.196–206.

Wahlström, J., Skog, I. and Händel, P.H. (2017) 'Smartphone-based vehicle telematics: a ten-year anniversary', *IEEE Transactions on Intelligent Transportation Systems*, Vol. 18, No. 10, pp.2802–2825.

World Health Organization (2013) *Global Status Report on Road Safety* [online] http://www.who.int/violence_injury_prevention/road_safety_status/2013/en/ (accessed August 2016).

Wu, M., Zhang, S. and Dong, Y. (2016) 'A novel model-based driving behavior recognition system using motion sensors', *Sensors*, Vol. 16, No. 10, pp.1746–1769.